Purification and Biophysical Characterization of a Minimal Functional Domain and of an N-Terminal Zn^{2+}-Binding Fragment from the Human Papillomavirus Type 16 E6 Protein†

Francesco Lipari, Graham A. McGibbon, Elizabeth Wardrop, and Michael G. Cordingley*

Department of Biological Sciences, Boehringer Ingelheim (Canada) Ltd., 2100 Cunard Street, Laval, Quebec, Canada H7S 2G5

Received August 4, 2000; Revised Manuscript Received December 1, 2000

ABSTRACT: The E6 Zn^{2+}-binding protein of high-risk human papillomaviruses (HPVs) is one of the major transforming proteins encoded by these tumor viruses. A bacterial system was used to express wild type and truncated forms of HPV-16 E6 linked to GST. The recombinant proteins were released from GST through cleavage of a factor Xa site. Functional analysis of these proteins demonstrated that amino acids 2−142 comprise the minimal domain of E6 required to promote the degradation of p53 in vitro in a rabbit reticulocyte lysate. This purified protein, E6(Δ143−151), required a high salt concentration for maximum solubility, eluted as a monomer on gel filtration, and was shown to bind two Zn^{2+} ions by atomic absorption analysis. An N-terminal subdomain of E6 (amino acids 2−77, E6-N) was similarly purified. Unlike E6(Δ143−151), E6-N was very soluble in low-salt buffers and hence was highly amenable to biophysical characterization. E6-N was shown to bind one Zn^{2+} ion by electrospray mass spectrometry and by atomic absorption analysis. UV−visible spectroscopic analysis of Co^{2+}-substituted E6-N revealed that four cysteine residues coordinate the metal ion. Mutational studies of all the cysteine residues in E6-N substantiated a critical role for Cys 30, 33, 63, and 66 in Zn^{2+} binding and in proper folding of the subdomain. Equilibrium sedimentation of E6-N demonstrated that it is a monomer, like E6(Δ143−151), at low concentrations, but dimerization occurs at high concentrations (K_d = 0.1 mM). Finally, circular dichroism studies revealed significant secondary structure for both E6(Δ143−151) and E6-N. The results support a model of monomeric E6 possessing two functionally critical Zn^{2+}-binding motifs.

The human papillomaviruses (HPVs)[1] are small DNA viruses that infect the upper layers of the skin or mucosa in a variety of locations (hands, feet, mouth, and genitalia) causing warts or papillomas. More than 80 virus types have been identified, and each type shows tropism for a particular body site. Approximately one-third of the HPVs specifically infect the anogenital region (*1*), and HPV has become one of the most prevalent sexually transmitted viral agents (*2*). The low-risk anogenital-specific viruses (e.g., types 6 and 11) cause only benign lesions, whereas the lesions caused by high-risk types (e.g., types 16 and 18) have the potential for progression to cancer. In fact, more than 90% of cervical carcinomas can be demonstrated to contain DNA from high-risk HPVs.

The high-risk HPVs encode two transforming proteins, E6 and E7, which are selectively retained and expressed in cervical carcinomas (*1*). These proteins can cooperate in the immortalization of cultured cells (*1*) and in the induction of tumors in transgenic mice (*3*). Even when expressed alone, E6 has transforming activities. For example, HPV-16 E6 has the ability to immortalize human mammary epithelial cells in culture (*4*), and epidermis-directed expression of this gene in transgenic mice caused malignant skin tumors (*5*).

A variety of studies have been performed to determine the mechanism by which E6 of high-risk viruses induces oncogenesis. The most well understood function, and probably one of the most important, is its ability to promote degradation of the p53 tumor suppressor protein. The inactivation of p53 occurs through formation of a complex between E6, E6-AP, which is a cellular ubiquitin ligase, and p53 (*6*). Formation of this complex results in ubiquitination of p53 and subsequent p53 degradation by the 26S proteosome. It has become evident, however, that E6 has p53-independent functions that may also play an important role in inducing carcinogenesis. High-risk E6 has been found to interact with CBP/p300, a transcriptional coactivator (*7*, *8*). E6 also binds to an ER Ca^{2+}-binding protein named E6-BP or ERC-55 (*9*), which may be a significant function since Ca^{2+} ions play an important role in cell proliferation. In addition, E6 is thought to disrupt the actin cytoskeleton through interaction with paxillin (*10*, *11*). The E6 oncoprotein also binds to interferon regulatory factor-3 and inhibits its transcriptional activity (*12*). Recently, an interaction was discovered between E6 and Tyk2, a tyrosine kinase important

† F.L. is the recipient of a postdoctoral fellowship from the Medical Research Council of Canada in partnership with Canada's Research-Based Pharmaceutical Companies.

* To whom correspondence should be addressed. Telephone: (450) 682-4640. Fax: (450) 682-4642. E-mail: mcordingley@lav.boehringer-ingelheim.com.

[1] Abbreviations: CD, circular dichroism; CSA, camphorsulfonic acid; DDM, *n*-dodecyl β-D-maltoside; DTT, dithiothreitol; EDTA, ethylenediaminetetraacetic acid; ES-MS, electrospray mass spectrometry; HPV, human papillomavirus; IPTG, isopropyl 1-thio-β-D-galactopyranoside; LB, Luria broth; SDS−PAGE, sodium dodecyl sulfate−polyacrylamide gel electrophoresis; TCEP, tris(carboxyethyl)phosphine.

10.1021/bi001837+ CCC: $20.00
Published on Web 01/12/2001

in the Jak-STAT signaling pathway (*13*). There are also reports of other important cellular proteins that are targeted for proteosome degradation through interaction with E6. These proteins include Myc (*14*), E6TP1 (*15*), Bak (*16*, *17*), and hDlg (*18*, *19*). Interestingly, all of the proteins mentioned that interact with high-risk E6 have a negligible or low affinity for the E6 proteins from low-risk HPV types.

The HPV E6 proteins are small proteins of about 150 amino acids in length. An alignment of the amino acid sequences of the different E6 proteins indicated that the most highly conserved portions of the molecules are two putative Zn^{2+}-binding regions (*20*). Each region contains a Cys-X_2-Cys-X_{29-30}-Cys-X_2-Cys motif whereby the four Cys residues are predicted to be the Zn^{2+}-ligating residues. The spacing of 29 or 30 amino acids between the two pairs of Cys residues is unique among CCCC fingers in which there are usually fewer than 20 amino acids separating the pairs of Cys residues (*21*). These regions were also proposed to be novel Zn^{2+}-binding structures from analysis of secondary structure predictions (*20*). However, to date there is no three-dimensional structure or biophysical data available to substantiate the secondary structure predictions. Furthermore, the Zn^{2+}-binding properties of E6 have been characterized only through observation of radioactive Zn^{2+} binding to E6 immobilized on membranes (*22*−*24*); therefore, quantitative measurement of Zn^{2+} was never performed.

The lack of biophysical data on purified E6 protein has hampered direct analysis of its quaternary structure. Indirect gel filtration analysis of radiolabeled E6 from a crude lysate indicated possible dimeric E6 (*25*), and cross-linking experiments of purified E6 revealed dimeric species (*26*). However, cross-linking experiments also demonstrated that monomeric E6 binds E6-AP to form a heterodimeric complex (*26*).

It is surprising that there is practically nothing known about the secondary, tertiary, or quaternary structure of E6 considering the importance of E6 as a viral oncoprotein. In this report, we describe the purification and structural characterization of two derivatives of the E6 protein from type 16 HPV. A C-terminal deletion mutant, E6(Δ143−151), which is functional in p53 degradation, and an N-terminal subdomain of E6 (up to amino acid 77) have been expressed in *Escherichia coli* and purified in milligram amounts using an efficient purification protocol. Our studies with these two variants of the E6 protein demonstrate that each is a Zn^{2+}-binding protein, with the E6 minimal functional domain, E6(Δ143−151), binding two Zn^{2+} ions, while the N-terminal subdomain binds a single Zn^{2+}. Both are folded, soluble proteins and contain significant α-helical and β-sheet structures as determined by circular dichroism studies, and both are monomeric at physiological concentrations. Mutational and spectroscopic studies define the Zn^{2+}-ligating Cys residues within the N-terminal subdomain and substantiate a critical role of these residues in metal binding and in proper folding of the protein subdomain. These data are consistent with the critical role of the Zn^{2+}-ligating Cys residues for the biological activities of the E6 protein (*4*, *22*).

EXPERIMENTAL PROCEDURES

Buffers. The following buffers were used: buffer A, 20 mM Tris (pH 7.5), 0.1 M NaCl, 0.2 mM EDTA, and 10 mM DTT; buffer B, 20 mM Tris (pH 7.5), 1.0 M NaCl, 0.2 mM EDTA, and 10 mM DTT; buffer C, 40 mM Tris (pH 8.0), 1.0 M NaCl, and 1 mM TCEP; buffer E, 10 mM Tris (pH 8.0), 0.1 M NaCl, and 1 mM TCEP; buffer G, 5 mM Tris (pH 8.0) and 0.1 mM TCEP; buffer H, 5 mM Tris (pH 8.0), 0.5 M NaF, and 0.1 mM TCEP; buffer Xa, 40 mM Tris (pH 8.0), 1 mM $CaCl_2$, 0.5 M NaCl, and 10 mM DTT; and buffer P, 25 mM Tris (pH 7.5), 0.1 M NaCl, and 3 mM DTT. For all buffers containing DTT, the DTT was added fresh from a 1 M stock. For buffers containing TCEP, the pH was adjusted after addition of TCEP.

Plasmid Construction. DNA plasmids containing the sequences for HPV-16 E6 and human p53 (Arg 72 type) (*27*) were kindly provided by G. Matlashewski (McGill University, Montreal, PQ). The sequence encoding p53 was amplified by PCR using a 5′ primer (CTTAAGCTTCGA-TCGTCGACTCTA) and a 3′ primer (CCCGGATCCTCAG-TCTGAGTCAGGCCCTTC), and this fragment was cloned into the vector PCR 3.1 (Invitrogen) using standard procedures. The sequences encoding different lengths of the E6 protein were generated by PCR and cloned into the pGEX-3X vector (Pharmacia) using standard molecular biology techniques. Site-directed mutagenesis was performed using the QuickChange site-directed mutagenesis kit (Stratagene). All sequences were verified by automated sequencing on an ABI PRISM 377 DNA sequencer (Applied Biosystems).

Expression of GST Fusion Proteins in E. coli. All proteins were expressed in *E. coli* strain BL21(DE3)pLysS (Novagen). Cultures were grown at 37 °C in LB containing 100 μg/mL ampicillin until an A_{600} of 0.6−1.0 had been reached and then transferred to 22−23 °C (250 rpm). After 45 min at 22−23 °C, recombinant protein production was induced with 0.1 mM IPTG for 3−20 h. Cells were collected by centrifugation and stored at −80 °C for at least 16 h before cell extracts were prepared. For the production of Co^{2+}-substituted E6-N, cultures were grown at 37 °C in the following medium: 33 mM Na_2HPO_4, 22 mM KH_2PO_4, 8 mM NaCl, 18 mM NH_4Cl, 2 mM $MgSO_4$, 3.6 g/L D-(+)-glucose, and 100 μg/mL ampicillin. Cultures were grown until the A_{600} reached ∼0.9 and then were transferred to 22 °C (250 rpm). After the mixture had been shaken for 45 min, IPTG and $CoCl_2$ were added to final concentrations of 0.1 and 0.04−0.1 mM, respectively. Protein production was induced for 18 h at 22 °C.

Preparation of N- and C-Terminal Deletion Mutants of E6 for the p53 Degradation Assay. Cell pellets from small-scale bacterial cultures (40−100 mL) expressing the GST fusion proteins were treated using a protocol similar to that described for the purification of E6(Δ143−151) (see the text below). Following factor Xa protease cleavage of the GST fusion proteins, the supernatants were separated from the beads by centrifugation and were analyzed on Coomassie-stained 15% SDS−PAGE gels. The concentration of E6 protein was measured by comparing the intensity of the E6 bands to that of the 20 kDa standard (Amersham Pharmacia Biotech) of which 0.25−1 μg was loaded.

Purification of E6(Δ143−151). For large-scale production of GST−E6(Δ143−151), cultures were grown in 2 L flasks (420 mL of LB per flask) and protein expression was induced for 20 h at 22 °C. Cell pellets from 2.5 L of culture were resuspended in 96 mL of buffer A containing 0.5 mg/mL DDM, and then 0.1% (v/v) Triton X-100, 10 mM $MgCl_2$, and 10 μg/mL deoxyribonuclease I from bovine pancreas

(Amersham Pharmacia Biotech) were added. The solution was gently rocked for 30 min and centrifuged for 40 min at 33000*g*, and then the supernatant was incubated with 10 mL of glutathione−Sepharose 4B beads (Amersham Pharmacia Biotech) for 1 h at room temperature with gentle rocking. The beads were then washed three times with 10 volumes of buffer B containing 0.5 mg/mL DDM followed by washing three times with 10 volumes of buffer Xa containing 0.5 mg/mL DDM. The washed beads were resuspended in an equal volume of buffer Xa containing 0.5 mg/mL DDM and 600 units of factor Xa protease (Amersham Pharmacia Biotech). After ~19 h at 4 °C with rocking, the reaction was terminated by addition of 20 μM factor Xa inhibitor (1,5-dansyl-Glu-Gly-Arg chloromethyl ketone, dihydrochloride, Calbiochem). The beads were washed with 3 volumes of buffer C containing 0.5 mg/mL DDM and 20 μM factor Xa inhibitor. The resulting protein solution was concentrated to less than 5.5 mL using Centriprep-30 centrifugal filters (Amicon). E6(Δ143−151) was then separated from the contaminating proteins using a Superdex-75 (16/60) FPLC column in buffer C. The purified protein was stored at −80 °C. All steps were performed at 4 °C unless indicated otherwise. For all wash steps, the beads were pelleted by centrifugation at 1500−2000*g* for 5 min and then resuspended in the appropriate buffer.

Purification of E6-N. E6-N was purified using a procedure similar to that used for E6(Δ143−151) with some modifications. None of the buffers contained DDM, and the cell extract was sonicated two times for 15 s each after resuspension in buffer A. Buffer Xa contained 0.25 M NaCl instead of 0.5 M NaCl, and the factor Xa protease reaction took 3 days instead of 19 h. The factor Xa inhibitor was not added to stop the cleavage reaction. Also, buffer C was replaced with buffer E, and a Centriprep-10 apparatus was used for concentration instead of a Centriprep-30.

p53 Degradation Assay. [^{35}S]Met-labeled p53 protein was produced using an in vitro rabbit reticulocyte lysate transcription−translation system (TNT, Promega) according to the manufacturer's instructions. For the p53 degradation assay, 5 μL of in vitro-translated p53 was mixed with 13.4 μL of buffer P and 1.6 μL (0.5−20 ng depending on the experiment) of recombinant E6. The mixture was incubated at ambient temperature, and 5 μL aliquots were removed after incubation for 0, 30, and 60 min. The aliquots were added to SDS−PAGE sample buffer and boiled to stop the reaction. Samples were analyzed using SDS−PAGE and autoradiography. The amount of p53 was determined using a phosphorimager (Molecular Dynamics, Inc.).

Atomic Absorption Spectrophotometry. Samples of purified E6(Δ143−151) and E6-N were analyzed for Zn^{2+} content using an atomic absorption spectrophotometer from Thermo Jarrell Ash (model Smith-Hieftje 11) at the Chemical Engineering Department (McGill University, Montreal, PQ). Zn^{2+} standards of 0−1 ppm were prepared in duplicate from a 1000 ppm calibrated stock solution (SPEX Certiprep, Inc.). The standards were prepared under conditions identical to those of the protein samples, and 1 mM EDTA was added to all samples and standards. The Zn^{2+} content of the buffers used was below detectable levels using the atomic absorption technique, which has a detection limit of about 0.05 ppm or 0.8 μM Zn^{2+}.

Analytical Ultracentrifugation. Sedimentation equilibrium experiments with E6-N were carried out at 20 °C in a Beckman Optima XL-A analytical ultracentrifuge with six-sector cells using three rotor speeds (25 000, 30 000, and 42 000 rpm) and three protein concentrations (0.5, 0.33, and 0.25 mg/mL). Absorbance measurements at 280 nm were taken in step mode with a radial step size of 0.003 cm. Five replicate measurements were taken at each step. Attainment of equilibrium was established by taking scans every 30−60 min until successive scans were invariant as determined using Match 7.0 (D. A. Yphantis and J. W. Lary, National Analytical Ultracentrifuge Center, Storrs, CT). Values for the reduced molecular mass, solvent density, and partial specific volume were calculated using Sednterp 1.00 (see ref *28* and D. B. Hayes, T. M. Laue, and J. Philo, University of New Hampshire, Durham, NH). Experimental data, obtained after equilibrium was reached, were analyzed using WinNonlin 1.050 (see ref *29* and D. A. Yphantis, J. W. Lary, and M. L. Johnson, National Analytical Ultracentrifuge Center) to determine the model that best fit the data and to calculate dissociation constants. The dissociation constants were calculated in absorbance units and then converted to molar units using the equation $K_d = 2/(K_{280}\epsilon_{280} \times 1.2)$, where K_{280} is the dissociation constant in absorbance units and ϵ_{280} is the extinction coefficient at 280 nm.

Circular Dichroism. CD spectra were obtained using a Jasco J-715 spectropolarimeter. The spectropolarimeter was calibrated before each use with CSA, and the value of the ratio of ellipticity for CSA at 290.5 and 192.5 nm was confirmed to be ≥2.0. Far-UV CD spectra were recorded using water-jacketed 1.0 or 0.1 mm path length cells (Hellma). A total of 10 accumulations were taken for each spectrum with a speed of 20 nm/min, a resolution of 0.5 nm, a response of 1 s, and a bandwidth of 1.0 nm. A water bath was used to maintain the temperature at 20 °C. Secondary structure was assessed using the self-consistent method (*30*) which is provided in the SOFTSEC software (Softwood Co.).

Electrospray Ionization Mass Spectrometry. Samples for ES-MS were prepared either under denaturing conditions in aqueous 30% acetonitrile and 1% acetic acid or under native conditions in 50 mM ammonium acetate (pH 7) (*31*). Buffer exchange was accomplished by repeated ultrafiltration in a Microcon-10 filter (Amicon). The protein concentrations were 10−20 and 50−100 μM for denatured and native samples, respectively. Samples were delivered at 10 μL/min by a Harvard Apparatus dual-syringe pump (model 11) from a glass 1.0 mL Hamilton Co. syringe. An aliquot of the analyte solution was injected via a Rheodyne 7125 instrument using a 10 μL loop. Electrospray mass spectra were obtained with a Quattro II mass spectrometer (Micromass) controlled by MassLynx 3.1 software. This software with the Maximum Entropy option was used for data acquisition and processing. Calibration was performed using the manufacturer's recommended NaI/CsI solution and verified against horse heart myoglobin (Sigma). For all experiments, the source temperature was 60 °C and the capillary voltage was 3.5 kV. For the denatured sample, the cone voltage was ramped from 27 to 69 V from *m*/*z* 300 to 2000, while for the nondenatured sample, the ramp was from 35 to 103 V from *m*/*z* 600 to 3320.

Table 1: p53 Degradation Activity of N- and C-Terminal Mutants of HPV-16 E6

E6	Sequence[a]	p53 degradation[b]
2-151	GI^{2}FQDPQERPRKLP……TGR**C**MS**C**CRSSRTRRETQ^{151}L	+
Δ1-7	GI^{8}RPRKLP……TGR**C**MS**C**CRSSRTRRETQ^{151}L	-
Δ1-12	GI^{13}P……TGR**C**MS**C**CRSSRTRRETQ^{151}L	-
Δ147-151	GI^{2}FQDPQERPRKLP……TGR**C**MS**C**CRSSRT^{146}R	+
Δ143-151	GI^{2}FQDPQERPRKLP……TGR**C**MS**C**CR^{142}S	+
Δ136-151	GI^{2}FQDPQERPRKLP……TG^{135}R	-

[a] The predicted sequence of the N- and C-terminal ends of the recombinant E6 proteins after factor Xa cleavage is illustrated. The superscript (top left) indicates the amino acid position in the 151-amino acid HPV-16 E6 protein sequence (*42*). Two putative Zn^{2+}-ligating Cys residues (Cys 136 and Cys 139) are highlighted (see also Figure 9). [b] GST fusion proteins were expressed in *E. coli* and purified on glutathione−Sepharose beads, and then E6 was cleaved away with factor Xa protease as described in detail in Experimental Procedures. Approximately 5−20 ng of E6 protein, free of GST, was assayed in the p53 degradation assay according to the method described in Experimental Procedures. A "+" indicates >90% degradation after incubation for 1 h, and a "−" indicates <10% degradation after incubation for 1 h.

Protein Analysis and Quantitation. SDS−PAGE under reducing conditions was carried out according to Laemmli (*32*) using the Bio-Rad Mini-Protean II apparatus. Tris-tricine SDS−PAGE for low-molecular mass polypeptides was performed according to the method of Schagger and von Jagow (*33*). Gels were stained with Coomassie brilliant blue R-250. The concentration of the purified protein was determined spectroscopically by absorbance at 280 nm using molar extinction coefficients of 9600 M^{-1} cm^{-1} for E6-N and 21 200 M^{-1} cm^{-1} for E6(Δ143−151), which were determined by quantitative amino acid analysis. Since Co^{2+}-substituted E6-N could not be quantitated spectroscopically, this protein was quantitated by densitometry following SYPRO Orange (Bio-Rad) staining of SDS−PAGE gels, using purified E6-N as the standard.

RESULTS

Expression of Recombinant HPV-16 E6 Mutants in E. coli. To obtain functional recombinant E6 for structural studies, an *E. coli* expression system was chosen whereby E6 (amino acids 2−151; see Table 1) was expressed as a GST fusion protein containing a cleavable factor Xa protease site. The fusion protein was expressed and purified on glutathione−Sepharose beads. Treatment with factor Xa protease while the fusion protein was bound to the glutathione−Sepharose beads resulted in release of soluble E6 into the supernatant. The recombinant E6 obtained using this protocol was assayed for its ability to induce degradation of p53 in vitro in a rabbit reticulocyte lysate, which contains all the components necessary for ubiquitin-mediated proteolysis. Approximately 5 ng of partially purified E6 was sufficient to observe degradation of p53. Unfortunately, the recombinant E6 was partially degraded during factor Xa protease treatment, resulting in lower-molecular mass species of 1−2 kDa smaller than the major E6 protein (data not shown). Factor Xa or a contaminating protease may have cleaved nonspecifically at flexible or unfolded portions of the protein (*34*).

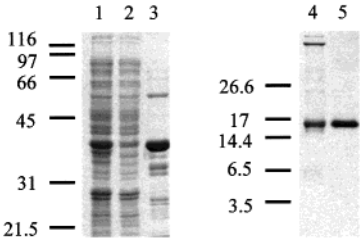

FIGURE 1: Purification of recombinant E6(Δ143−151). Samples from different purification steps were analyzed by 12.5% (lanes 1−3) or Tris-tricine (lanes 4 and 5) SDS−PAGE gels stained with Coomassie: lane 1, cellular extract; lane 2, cellular extract after centrifugation at 33000*g* for 40 min; lane 3, GST fusion protein bound to glutathione beads; lane 4, sample subjected to Superdex-75 chromatography; and lane 5, 2 μg of purified recombinant E6-(Δ143−151) after Superdex-75 chromatography. The molecular size markers (kilodaltons) (Bio-Rad) are indicated in the left margins.

Therefore, obtaining a homogeneous protein from this preparation of full-length E6 would necessitate additional purification steps, and would provide a considerably lower yield and increase the time for purification.

To facilitate purification and to remove the N- or C-terminal unstructured regions that may be susceptible to proteolysis and deleterious to further structural determination such as crystallization (*35*), N- and C-terminal truncation mutants were constructed (Table 1). These mutants were tested in the p53 degradation assay to determine if they retained their function. Deletion of the first seven residues of E6 resulted in a greater than 10-fold decrease in p53 degradation activity for E6(Δ1−7) compared to that for E6-(2−151). Removal of five, E6(Δ147−151), or nine, E6-(Δ143−151), residues from the C-terminal end of E6 resulted in p53 degradation activity for these mutants that was very similar to the activity of E6(2−151). Basically, more than 90% degradation of p53 was observed after incubation for 1 h with about 5 ng of protein. However, deleting further from the C-terminal end, E6(Δ136−151), resulted in a greater than 10-fold decrease in p53 degradation activity. Since the truncated E6 protein, E6(Δ143−151), was the shortest protein that retained the ability to induce p53 degradation and could be efficiently produced in *E. coli*, we focused on this protein for further characterization.

Purification and Characterization of E6(Δ143−151). E6(Δ143−151), constituting the minimal functional domain of E6, was purified with only one affinity chromatography step and one size exclusion chromatography step (Figure 1). Less than 10% of the fusion protein was recovered from the cellular extract after centrifugation (compare lanes 1 and 2); however, due to the high expression level, the yield of fusion protein was about 10 mg/L of bacterial culture. The GST fusion protein, with an expected molecular mass of 43 kDa, was the major protein bound to the beads (lane 3). Different factor Xa cleavage conditions were tested for cleavage of the fusion protein, and it was found that 0.5 M NaCl in the buffer was required for the optimal yield of soluble E6. Following cleavage of the fusion protein with factor Xa protease, the major protein found in the supernatant was E6-(Δ143−151) (17 kDa, lane 4). Size exclusion chromatography provided highly pure E6(Δ143−151) (lane 5) with only one band observed on SDS−PAGE and a yield of about 0.5 mg/L. Therefore, expressing a C-terminal truncation mutant of E6 was a successful strategy for obtaining a

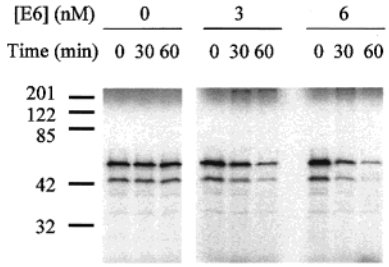

FIGURE 2: Activity of E6(Δ143−151) in p53 degradation. Purified E6(Δ143−151) was diluted appropriately in buffer C containing 0.1 mg/mL bovine serum albumin and then assayed in the in vitro p53 degradation assay according to the method described in Experimental Procedures. Autoradiograms of the SDS−PAGE gels used for separation of the ^{35}S-labeled p53 are shown. The molecular size markers (kilodaltons) (Bio-Rad) are indicated in the left margin.

homogeneous E6 protein. The yield was substantially lower than the expected yield of about 5 mg/L based on the amount of fusion protein that was obtained. A major loss of E6-(Δ143−151) occurred due to aggregation and nonspecific binding to surfaces during purification.

The availability of the purified E6(Δ143−151) protein allowed for an accurate measure of its concentration and activity in the in vitro p53 degradation assay (Figure 2). Only 3 nM (0.05 ng/μL) protein was required to promote 50 and 80% degradation of p53 after 30 and 60 min, respectively. With 6 nM (0.1 ng/μL) protein, the reaction was 75 and 95% complete after 30 and 60 min, respectively. Degradation was also observed using 1.5 nM (0.025 ng/μL) protein, with about 50% degradation observed after incubation for 1 h (data not shown). These concentrations of E6(Δ143−151) required to observe activity correlate very well with our estimate that approximately 1 nM in vitro-translated full-length E6 is required to observe p53 degradation under similar assay conditions in which there was approximately 2 nM p53 (data not shown). Hence, the purified E6(Δ143−151) is highly active in promoting p53 degradation and has activity similar to that of full-length E6.

The biochemical and structural properties of E6(Δ143−151) were further characterized. ES-MS analysis under denaturing conditions (aqueous 30% acetonitrile and 1% acetic acid) of purified E6(Δ143−151) indicated a mass of 17 242 Da, which is very close to the expected mass of 17 245 Da. To determine the Zn^{2+} content of the purified protein, atomic absorption analysis was performed on the native protein obtained directly from the size exclusion column. The purified protein contained 1.8 ± 0.1 Zn^{2+} ions per molecule. To determine the oligomerization status of the purified protein at different salt concentrations, it was subjected to analytical size exclusion chromatography on Superdex-75 using 0.1, 0.3, and 1.0 M NaCl-containing buffer (Figure 3). E6(Δ143−151) eluted at about 14 kDa under all the conditions that were tested, which is very close to the expected monomer molecular mass of 17 kDa. The protein was not highly soluble in the buffer containing 0.1 M NaCl and seemed to adhere to the gel filtration column, resulting in an asymmetrical peak. Circular dichroism was performed (Figure 4) with the protein in a buffer containing 0.5 M NaF to keep it soluble. Analysis of the spectrum using the self-consistent method provided an estimation of the secondary structure of the protein: 26% α-helix, 27% β-sheet, and 24% turns.

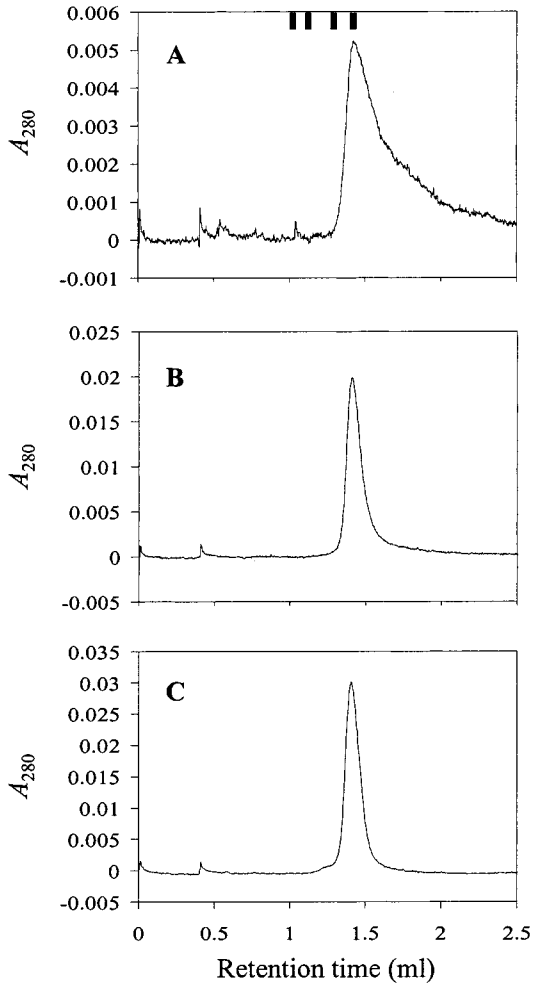

FIGURE 3: Size exclusion chromatography of purified E6(Δ143−151). Samples of purified E6(Δ143−151) were analyzed on a Superdex-75 (PC 3.2/30) column using the SMART System (Pharmacia). Chromatography was performed in 40 mM Tris (pH 8.0) and 1 mM TCEP containing different concentrations of NaCl: (A) 0.1 M, (B) 0.3 M, and (C) 1.0 M. The purified protein was prepared in the different buffers at a concentration of 1−2 (A) or 5−10 μM (B and C), and then 50 μL was injected onto the column. The four vertical bars in panel A denote the positions of the molecular size standards (Amersham Pharmacia Biotech) and correspond, from left to right, to bovine serum albumin (66 kDa), chymotrypsinogen (45 kDa), ovalbumin (25 kDa), and ribonuclease A (14 kDa).

Purification and Characterization of E6-N. Further structural analysis of E6(Δ143−151) was hampered by relatively poor solubility; therefore, we considered that dissection of the protein into subdomain peptides might provide an avenue for further structural characterization studies. In fact, during the purification of E6(Δ143−151), nonspecific proteolysis of the protein produced a low-molecular mass protein which migrated between 6 and 10 kDa on SDS−PAGE (data not shown). N-Terminal sequencing and ES-MS analysis of the proteolytic fragment indicated that it corresponded to the N-terminal half of E6(Δ143−151) ending at amino acid 77 (data not shown). To expedite purification of this soluble subdomain for further characterization, a new construct was made expressing amino acids 2−77 of E6 linked to GST. As for E6(Δ143−151), the N-terminal sequence after factor Xa cleavage was GI^{2}FQDP. The protein, named E6-N, was purified (Figure 5) using a protocol very similar to that used for E6(Δ143−151). More than 50% of the GST fusion

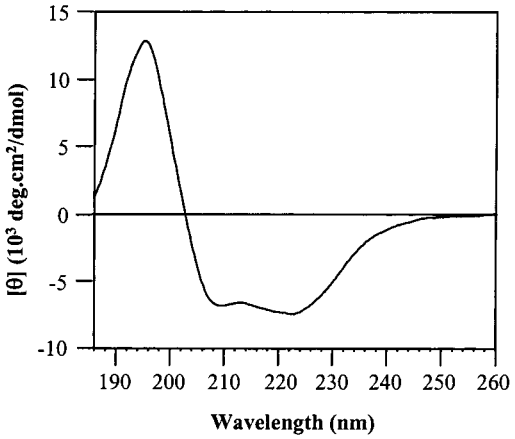

FIGURE 4: Circular dichroism spectrum of E6(Δ143−151). Purified E6(Δ143−151) was exchanged to buffer H using a NAP-10 column (Amersham Pharmacia Biotech). The CD spectrum of 5 μM (0.09 mg/mL) E6(Δ143−151) was then measured in a 1.0 mm cell according to the method described in Experimental Procedures.

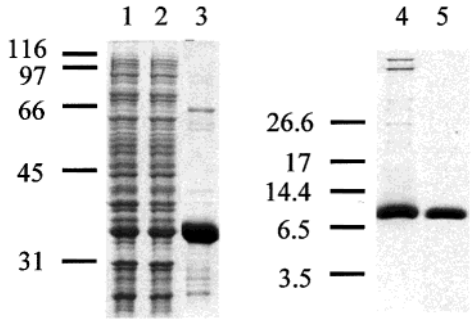

FIGURE 5: Purification of E6-N. Samples from different purification steps were analyzed by 12.5% (lanes 1−3) or Tris-tricine (lanes 4 and 5) SDS−PAGE gels stained with Coomassie: lane 1, cellular extract; lane 2, cellular extract after centrifugation at 33000*g* for 40 min; lane 3, GST fusion protein bound to glutathione beads; lane 4, sample subjected to Superdex-75 chromatography; and lane 5, 1.4 μg of purified recombinant E6-N after Superdex-75 chromatography. The molecular size markers (kilodaltons) (Bio-Rad) are indicated in the left margins.

protein (35 kDa) was recovered from the cellular extract after centrifugation (compare lanes 1 and 2). E6-N (9.4 kDa) was the major protein in the supernatant after factor Xa protease cleavage of the fusion protein (lanes 3 and 4). Size exclusion chromatography produced highly pure E6-N (lane 5) with an excellent yield of about 10 mg/L.

E6-N is a highly soluble protein. For example, concentrations up to 10 mg/mL could be attained in 10 mM Tris buffer (pH 8.0) containing 0.1 M NaCl and 1 mM TCEP. The high solubility of this protein made it more ideal for biophysical studies. It was first analyzed for Zn^{2+} by atomic absorption analysis, which indicated a Zn^{2+} content of 0.95 ± 0.06 ion per protein molecule. ES-MS analysis of the protein in ammonium acetate buffer gave a mass of 9462.5 Da, which is very close to the predicted molecular mass of the protein containing one Zn^{2+} ion (9461.3 Da).

Size exclusion chromatography indicated that the protein may oligomerize in a salt-dependent fashion (data not shown), and therefore, equilibrium sedimentation experiments were performed at two different salt concentrations to analyze the oligomerization characteristics of this Zn^{2+}-binding domain (Figure 6). Analysis of the equilibrium data indicated that a monomer−dimer equilibrium was the best

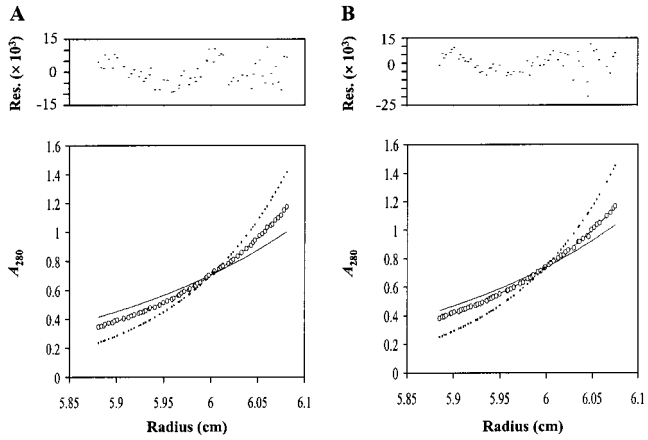

FIGURE 6: Equilibrium sedimentation of E6-N. Equilibrium sedimentation was performed according to the method described in Experimental Procedures using 10 mM Tris (pH 8.0) and 1 mM TCEP buffer containing different concentrations of NaCl: (A) 0.1 and (B) 0.3 M. Only the data at 25 000 rpm and 53 μM (0.5 mg/mL) protein are represented. The experimental data, represented as white circles, were truncated at 1.2 absorbance units. Lines representing the theoretical fit for a monomer−dimer equilibrium are mostly covered by the experimental data. Solid and dotted lines represent the theoretical fit for monomer and dimer models, respectively. The parameters used to calculate the theoretical curves were obtained by linking the data from all speeds and protein concentrations. The residuals (Res.) represent the difference between the theoretical and experimental data at 25 000 rpm.

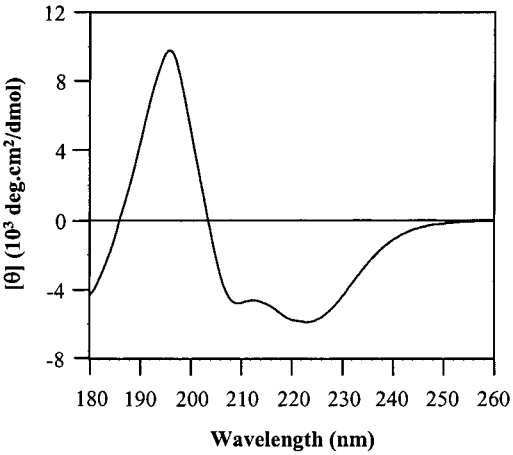

FIGURE 7: Circular dichroism spectrum of E6-N. Purified E6-N was dialyzed overnight at 4 °C in buffer G. The CD spectrum was measured at a protein concentration of 163 μM (1.53 mg/mL) in a 0.1 mm cell according to the method described in Experimental Procedures.

fit to the data. Similar values for the dissociation constants were obtained when each speed and protein concentration was analyzed separately at a given salt concentration. Altogether, the data from nine experiments (three speeds with three different protein concentrations) were linked, and the value for the reduced molecular mass was fixed to determine an average value for the dissociation constant. At 0.1 M NaCl, the protein formed a dimer with a K_d of 0.11 mM (95% confidence limits of 0.09 and 0.14 mM), but the affinity decreased at 0.3 M NaCl to a K_d value of 0.22 mM (95% confidence limits of 0.17 and 0.28 mM).

Circular dichroism was used to investigate the secondary structure of E6-N (Figure 7). Analysis of the spectrum using the self-consistent method provided an estimation of the secondary structure of the protein: 25% α-helix, 29%

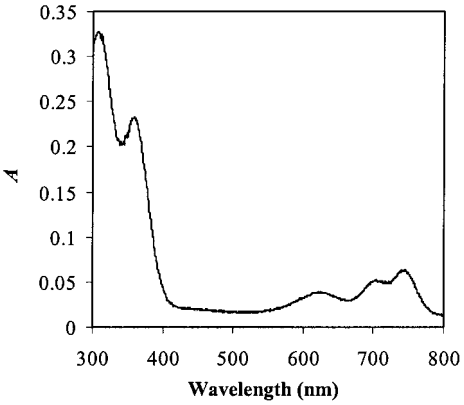

FIGURE 8: Electronic absorption spectrum of Co^{2+}-substituted E6-N. Purified Co^{2+}-substituted E6-N was concentrated to 50 μM, and the spectrum was recorded using a quartz cuvette with a path length of 1 cm. The spectrum of the buffer (buffer E) was subtracted.

β-sheet, and 25% turns. Collectively, these results indicated that the N-terminal half of E6 can fold and bind Zn^{2+} independently of the remaining C-terminal half of the protein.

Identification of the Zn^{2+}-Ligating Residues in E6-N. To identify the Zn^{2+}-ligating residues in E6-N, we began by investigating the coordination environment of the Zn^{2+} ion. Zn^{2+} was substituted with Co^{2+} using biosynthetic incorporation, and the Co^{2+}-substituted E6-N was purified using the same protocol that was used for E6-N. Atomic absorption analysis confirmed that the purified E6-N contained one bound Co^{2+} per molecule (data not shown). The electronic absorption spectrum of Co^{2+}-substituted E6-N illustrated in Figure 8 shows that two Co−S charge transfer bands are present at 305 and 360 nm and three Co^{2+} d−d transition bands are present at 620, 700, and 740 nm. The fact that the d−d transition bands extend as far as 740 nm is indicative of a CoS_4 complex (*36*). The spectrum therefore demonstrates that there are four Cys residues binding to the Co^{2+} ion.

E6-N contains six Cys residues, four of which are invariant in the family of E6 proteins and have been predicted to ligate Zn^{2+} (Figure 9). In an attempt to confirm that Cys 30, 33, 63, and 66 are actually coordinating the Zn^{2+} ion, each residue was mutated individually to Ser in the GST−E6-N fusion protein and the proteins were expressed in bacteria. All four mutant fusion proteins were highly insoluble in bacteria, and none of the mutant E6-N proteins could be purified in a quantity adequate for Zn^{2+} analysis. The other two Cys residues, Cys 16 and Cys 51, were also mutated to Ser. These mutant E6-N proteins were soluble and were purified using the same protocol that was used for wild type E6-N. The C16S and C51S mutant proteins bound 1 equiv of Zn^{2+} as observed using atomic absorption analysis (data not shown).

DISCUSSION

A minimal functional domain of HPV-16 E6, E6(Δ143−151), was identified by analyzing N- and C-terminal truncation mutants and has been efficiently produced and purified in milligram amounts. It was found that the seven N-terminal amino acids of E6 are essential for its activity in promoting p53 degradation, which is consistent with a previous study in which an F2V mutant of in vitro-translated E6 was no longer functional in p53 degradation (*37*). These results

A

```
                          16                  30 33
16E6   MFQDPQERPRKLPQLCTELQTTIHDIILECVYCKQQLL 38
18E6 MARFEDPTRRPYKLPDLCTELNTSLQDIEITCVYCKTVLE 40
6aE6  MESANASTSATTIDQLCKTFNLSMHTLQINCVFCKNALT 39
11E6  MESKDASTSATSIDQLCKTFNLSLHTLQIQCVFCRNALT 39

                  51              63 66
16E6 RREVYDFAFRDLCIVYRDGNPYAVCDKCLKFYSKISEYRH 78
18E6 LTEVFEFAFKDLFVVYRDSIPHAACHKCIDFYSRIRELRH 80
6aE6 TAEIYSYAYKQLKVLFRGGYPYAACACCLEFHGKINQYRH 79
11E6 TAEIYAYAYKNLKVVWRDNFPFAACACCLELQGKINQYRH 79

16E6 YCYSLYGTTLEQQYNKPLCDLLIRCINCQKPLCPEEKQRH 118
18E6 YSDSVYGDTLEKLTNTGLYNLLIRCLRCQKPLNPAEKLRH 120
6aE6 FDYAGYATTVEEETKQDILDVLIRCYLCHKPLCEVEKVKH 119
11E6 FNYAAYAPTVEEETNEDILKVLIRCYLCHKPLCEIEKLKH 119

16E6 LDKKQRFHNIRGRWTGRCMSCCRSSR-----TRRETQL   151
18E6 LNEKRRFHNIAGHYRGQCHSCCNRARQERLQRRRETQV   158
6aE6 ILTKARFIKLNCTWKGRCLHCWTTCM--------EDMLP  150
11E6 ILGKARFIKLNNQWKGRCLHCWTTCM--------EDLLP  150
```

B

```
E6(Δ143-151)  GIFQDPQERPRKLPQLCTELQTTIHDIILE  29
              CVYCKQQLLRREVYDFAFRDLCIVYRDGNP  59
              YAVCDKCLKFYSKISEYRHYCYSLYGTTLE  89
              QQYNKPLCDLLIRCINCQKPLCPEEKQRHL  119
              DKKQRFHNIRGRWTGRCMSCCRS         142

E6-N  GIFQDPQERPRKLPQLCTELQTTIHDIILECVYCKQ  35
      QLLRREVYDFAFRDLCIVYRDGNPYAVCDKCLKFYS  71
      KISEYR                                77
```

FIGURE 9: Alignment of HPV E6 proteins. (A) The amino acid sequences of the E6 proteins from HPV types 16, 18, 6a, and 11 were aligned. The eight Cys residues that are invariant among all of the HPV E6 proteins (*20*) are highlighted with a box. The Cys residues that have been mutated to Ser in E6-N are numbered. (B) The amino acid sequences of E6(Δ143−151) and E6-N are illustrated. The first two residues, GI, are not considered in the numbering of the amino acids; therefore, F is amino acid number 2 as in the wild type HPV type 16 E6 sequence shown in panel A.

demonstrate the importance of the N-terminus for activity. On the other hand, up to nine residues could be removed from the C-terminus without any loss of function. This result is consistent with two other studies of E6 mutants. In one study, it was demonstrated that a Δ142−149 deletion mutant of E6 expressed in vitro retained p53 degradation function (*38*). Similarly, the second study indicated that both Δ140−151 and Δ146−151 mutants of E6 retained close to normal p53 degradation activity when expressed either in vitro or in vivo in mammalian cells (*39*). Our results further indicated that truncation of the C-terminus to remove two putative Zn^{2+}-ligating Cys residues (Cys 136 and Cys 139) in the E6(Δ136−151) mutant resulted in a dramatic loss of p53 degradation activity. Our result is consistent with a previous study in which a Δ136−151 mutant of E6 was not stable when expressed either in vitro or in vivo in mammalian cells (*39*). In conclusion, our results are consistent with previous studies of truncation mutants and have confirmed the minimal domain of E6 required for p53 degradation. The good correlation between our results and those of others supports the conclusion that our purified E6 protein is as active as E6 produced by in vitro translation or assayed in transfected cells.

In this study, we found that the N-terminal half of E6 is an independently folded Zn^{2+}-binding subdomain. Previous

mutagenesis studies (*38*−*41*) of residues in the N-terminal half of E6 indicated that this part of the protein plays an essential role in p53 degradation. It may be important for interaction with E6-AP in the initial heterodimer formation and may also be important for the interaction with p53 upon formation of the complex. The availability of purified E6-N allowed us to investigate its possible interactions with E6-AP and p53. In an in vitro binding assay, no interaction was observed between the GST−E6-N fusion protein and E6-AP or p53 (unpublished results). Furthermore, addition of E6-N to an in vitro degradation assay containing 6 nM E6(Δ143−151) resulted in inhibition of p53 degradation only at very high concentrations of E6-N (>50 μM) (unpublished results). These results indicate that the N-terminal half of E6 alone does not form significant interactions with E6-AP or p53. It is possible that multiple interactions throughout the E6 sequence are required for complex formation and p53 degradation.

The availability of purified proteins has allowed us to investigate for the first time the stoichiometry of Zn^{2+} binding to E6, the identity of Zn^{2+}-ligating residues, and the secondary structure of the protein. As demonstrated by atomic absorption and ES-MS analysis, E6(Δ143−151) binds 2 equiv of Zn^{2+} and E6-N binds 1 equiv. When the fact that Zn^{2+} was not added to any of the buffers during the purification protocol is considered, it can be concluded that E6(Δ143−151) and E6-N bind Zn^{2+} with a high affinity. The secondary structure content of E6(Δ143−151) (26% α-helix and 27% β-sheet) is consistent with the published prediction of 26% α-helix and 28% β-sheet. Similarly, our measurements for E6-N indicate that it contains about 25% α-helix and 29% β-sheet, also in close agreement with the published prediction of 23% α-helix and 30% β-sheet for this part of the protein (*20*). Our data therefore provide direct experimental evidence demonstrating that E6 contains two Zn^{2+}-finger motifs, each containing α-helix and β-sheet structures. The absorption spectrum of Co^{2+}-substituted E6-N indicates that four Cys residues coordinate the Zn^{2+} ion. Mutation of Cys 30, 33, 63, or 66 results in insoluble E6-N, whereas mutation of the remaining Cys residues, Cys 16 and 51, does not affect solubility or Zn^{2+} binding. Therefore, these results suggest that Cys 30, 33, 63, and 66 are the Zn^{2+}-ligating residues and that Zn^{2+} binding is required for the expression of soluble E6-N. Further evidence suggesting that the Zn^{2+} ion plays a structural role came from dialysis experiments which showed that treatment with EDTA at pH 5.5 results in complete precipitation of E6-N (unpublished results). Taken together, these results strongly suggest that the Zn^{2+} ion is ligated by Cys 30, 33, 63, and 66 and that metal binding is crucial to E6-N attaining its proper conformation.

Previous work has demonstrated that two of the Cys residues shown here to be crucial for Zn^{2+} binding were also essential for various aspects of E6 function. Mutation of Cys 63 in HPV-16 E6 greatly reduced the ability of the protein to induce p53 degradation and also abrogated its capacity to immortalize mammary epithelial cells (*4*). Another study showed that mutation of Cys 66 in HPV-16 E6 eliminated the ability of E6 to cooperate with E7 in the transformation of rat 3Y1 cells (*22*). Our data now indicate that the loss of function of these Cys mutants is due to improper folding of the E6 proteins.

In contrast to E6-N, E6(Δ143−151) is poorly soluble and highly sensitive to aggregation. These findings suggest that the C-terminal half of E6(Δ143−151) contributes to its poor solubility as a purified protein. Further evidence to support this hypothesis came from the observation that the C-terminal half of E6 was not recovered as a proteolytic degradation product after factor Xa digestion even though the N-terminal half was clearly present. Perhaps the C-terminal half was unstable or insoluble upon release from the N-terminal half. Although the C-terminal half of the protein contributes to the instability and insolubility of E6, Zn^{2+} analysis and circular dichroism data of E6(Δ143−151) indicate that the C-terminal half binds Zn^{2+} and is structured when it is part of this functional protein.

The availability of purified E6 allowed us to reexamine the quaternary structure of the protein. E6(Δ143−151) is monomeric at protein concentrations of 1−10 μM and in 0.1−1.0 M NaCl as observed by size exclusion chromatography. Unfortunately, this protein could not be studied by analytical ultracentrifugation because of its propensity to precipitate in the cells used for these experiments. In contrast, E6-N could be studied by equilibrium sedimentation and was shown to form dimers, but only at high protein concentrations (>0.1 mM). Collectively, our results indicate that E6 is a monomer at physiological concentrations and that monomeric E6 is functioning to induce degradation of p53. These results are consistent with previous work (*26*) showing that full-length HPV-16 E6 forms a heterodimeric complex with E6-AP.

This is the first publication describing structural studies of HPV E6 using a purified protein. Our results support a model of two functionally important Zn^{2+}-finger motifs in monomeric E6 and also substantiate the prediction that E6 represents a novel protein fold (*20*). The binding of Zn^{2+} by E6 is crucial to the protein attaining its appropriate folded conformation and maintaining its biological activities. E6(Δ143−151) and E6-N are ideal candidates for future studies that may shed light on more detailed aspects of E6 function and its interactions with protein binding partners such as E6-AP and p53. Furthermore, since there is significant homology between the E6 proteins from all HPV types, the structural information acquired for high-risk E6 is pertinent to all E6 proteins.

ACKNOWLEDGMENT

We thank Peter White for his help with analytical ultracentrifugation and circular dichroism experiments. We thank Jacques Archambault for helpful discussions and critical reading of the manuscript.

REFERENCES

1. Laimins, L. A. (1993) *Infect. Agents Dis. 2*, 74−86.
2. Phelps, W. C., Barnes, J. A., and Lobe, D. C. (1998) *Antiviral Chem. Chemother. 9*, 359−377.
3. Griep, A. E., Herber, R., Jeon, S., Lohse, J. K., Dubielzig, R. R., and Lambert, P. F. (1993) *J. Virol. 67*, 1373−1384.
4. Dalal, S., Gao, Q., Androphy, E. J., and Band, V. (1996) *J. Virol. 70*, 683−688.
5. Song, S., Pitot, H. C., and Lambert, P. F. (1999) *J. Virol. 73*, 5887−5893.
6. Huibregtse, J. M., Scheffner, M., and Howley, P. M. (1991) *EMBO J. 10*, 4129−4135.

7. Zimmerman, H., Degenkolbe, R., Bernard, H.-U., and O'Connor, M. J. (1999) *J. Virol. 73*, 6209−6219.
8. Patel, D., Huang, S.-M., Baglia, L. A., and McCance, D. J. (1999) *EMBO J. 18*, 5061−5072.
9. Chen, J. J., Hong, Y., Rustamzadeh, E., Baleja, J. D., and Androphy, E. J. (1998) *J. Biol. Chem. 273*, 13537−13544.
10. Tong, X., and Howley, P. M. (1997) *Proc. Natl. Acad. Sci. U.S.A. 94*, 4412−4417.
11. Vande Pol, S. B., Brown, M. C., and Turner, C. E. (1998) *Oncogene 16*, 43−52.
12. Ronco, L. V., Karpova, A. Y., Vidal, M., and Howley, P. M. (1998) *Genes Dev. 12*, 2061−2072.
13. Li, S., Labrecque, S., Gauzzi, M. C., Cuddihy, A. R., Wong, A. H. T., Pellegrini, S., Matlashewski, G. J., and Koromilas, A. E. (1999) *Oncogene 18*, 5727−5737.
14. Gross-Mesilaty, S., Reinstein, E., Bercovich, B., Tobias, K. E., Schwartz, A. L., Kahana, C., and Ciechanover, A. (1998) *Proc. Natl. Acad. Sci. U.S.A. 95*, 8058−8063.
15. Gao, Q., Srinivasan, S., Boyer, S. N., Wazer, D. E., and Band, V. (1999) *Mol. Cell. Biol. 19*, 733−744.
16. Thomas, M., and Banks, L. (1999) *J. Gen. Virol. 80*, 1513−1517.
17. Thomas, M., and Banks, L. (1998) *Oncogene 17*, 2943−2954.
18. Kiyono, T., Hiraiwa, A., Fujita, M., Hayashi, Y., Akiyama, T., and Ishibashi, M. (1997) *Proc. Natl. Acad. Sci. U.S.A. 94*, 11612−11616.
19. Gardiol, D., Kühne, C., Glaunsinger, B., Lee, S. S., Javier, R., and Banks, L. (1999) *Oncogene 18*, 5487−5496.
20. Ullman, C. G., Haris, P. I., Galloway, D. A., Emery, V. C., and Perkins, S. J. (1996) *Biochem. J. 319*, 229−239.
21. Berg, J. M., and Shi, Y. (1996) *Science 271*, 1081−1085.
22. Kanda, T., Watanabe, S., Zanma, S., Sato, H., Furuno, A., and Yoshiike, K. (1991) *Virology 185*, 536−543.
23. Grossman, S. R., and Laimins, L. A. (1989) *Oncogene 4*, 1089−1093.
24. Barbosa, M. S., Lowy, D. R., and Schiller, J. T. (1989) *J. Virol. 63*, 1404−1407.
25. Medcalf, E. A., and Milner, J. (1993) *Oncogene 8*, 2847−2851.
26. Daniels, P. R., Sanders, C. M., Coulson, P., and Maitland, N. J. (1997) *FEBS Lett. 416*, 6−10.
27. Matlashewski, G. J., Tuck, S., Pim, D., Lamb, P., Schneider, J., and Crawford, L. V. (1987) *Mol. Cell. Biol. 7*, 961−963.
28. Laue, T. M., Shah, B. D., Ridgeway, T. M., and Pelletier, S. L. (1992) in *Analytical Ultracentrifugation in Biochemistry and Polymer Science* (Harding, S. E., Rowe, A. J., and Horton, J. C., Eds.) pp 90−125, Royal Society of Chemistry, London.
29. Johnson, M. L., Correia, J. J., Yphantis, D. A., and Halvorson, H. R. (1981) *Biophys. J. 36*, 575−588.
30. Sreerama, N., and Woody, R. W. (1993) *Anal. Biochem. 209*, 32−44.
31. Loo, J. A., Holler, T. P., Foltin, S. K., McConnell, P., Banotai, C. A., Horne, N. M., Mueller, W. T., Stevenson, T. I., and Mack, D. P. (1998) *Proteins Suppl. 2*, 28−37.
32. Laemmli, U. K. (1970) *Nature 227*, 680−685.
33. Schagger, H., and von Jagow, G. (1987) *Anal. Biochem. 166*, 368−379.
34. LaVallie, E. R., and McCoy, J. M. (1994) in *Current Protocols in Molecular Biology* (Ausebel, F. M., Brent, R., Kingston, R. E., Moore, D. D., Seidman, J. G., Smith, J. A., and Struhl, K., Eds.) p 16.4.15, Wiley & Sons, New York.
35. McPherson, A. (1982) *Preparation and analysis of protein crystals*, Wiley & Sons, New York.
36. Maret, W., and Vallee, B. L. (1993) *Methods Enzymol. 226*, 52−59.
37. Liu, Y., Chen, J. J., Gao, Q., Dalal, S., Hong, Y., Mansur, C. P., Band, V., and Androphy, E. J. (1999) *J. Virol. 73*, 7297−7307.
38. Elbel, M., Carl, S., Spaderna, S., and Iftner, T. (1997) *Virology 239*, 132−149.
39. Foster, S. A., Demers, G. W., Etscheid, B. G., and Galloway, D. A. (1994) *J. Virol. 68*, 5698−5705.
40. Slebos, R. J. C., Kessis, T. D., Chen, A. W., Han, S. M., Hedrick, L., and Cho, K. R. (1995) *Virology 208*, 111−120.
41. Nakagawa, S., Watanabe, S., Yoshikawa, H., Taketani, Y., Yoshiike, K., and Kanda, T. (1995) *Virology 212*, 535−542.
42. Seedorf, K., Krämmer, G., Dürst, M., Suhai, S., and Röwekamp, W. G. (1985) *Virology 145*, 181−185.

BI001837+